Progress In Electromagnetics Research Letters, Vol. 112, 119–126, 2023

Efficient ADE-TLM Scheme for Modeling Drude Based Graphene in Terahertz Spectrum

Mohamed Moumou*, Soufiane El Adraoui, Khalid Mounirh, Mohammed Kanjaa, and Mohsine Khalladi

Abstract—In this work, a novel time domain Transmission Line Matrix (TLM) algorithm with Symmetrical Condensed Node (SCN) is developed to model electromagnetic (EM) wave propagation through a single graphene layer in Terahertz (THz) spectrum. The intraband conductivity of graphene (assumed to follow the Drude model) is implemented in TLM method by using the Auxiliary Differential Equation (ADE) of conduction current density. The validity and stability of the obtained results demonstrate the effectiveness and precision of this new modeling technique named ADE-(SCN)TLM, and prove that this method is a powerful tool that can be used to model and simulate complex devices based on graphene sheet for terahertz applications (e.g., Electronics, optoelectronic, etc.)

1. INTRODUCTION

Graphene, a single layer of graphite, discovered in 2004 [1], is one of the few 2D materials that is stable at room temperature (i.e., 300 K) and has unique properties due to its carbon atoms sp^2 hybridization. Among these properties, we cite high electrical conductivity, high current density, very high electron mobility, low optical absorption, high thermal conductivity, mechanical flexibility, etc. [2]. Graphene is described by several analytical complex surface conductivity models obtained by using quantum mechanics equations. Because of its unique electronic band structure, graphene's electrons act as massless relativistic particles (massless Dirac fermion) [3].

In order to simulate wave interaction with graphene sheet and investigate its electromagnetic property, Maxwell equations must be solved. For only a few case problems, Maxwell's equations have analytical solutions, and numerical solutions by using numerical methods are inevitable.

To analyze electromagnetic wave interactions on graphene sheet, numerical methods model graphene sheet layer as a thin surface with frequency dependent and dispersive conductivity, among these computational electromagnetic methods (CEMs), we have time domain numerical methods based on volumetric discretization as finite difference method (FDTD) and transmission line matrix method (TLM).

In the literature, two approaches are used for EM modeling of graphene layer by using the FDTD method, in the first approach, graphene layer can be seen as a thin layer with assumed non-zero thickness [4, 5], and in the second approach it is considered with practically zero thickness (i.e., as a Surface Boundary Condition [SBC]) [6–9].

In several publications, wave propagation through a dispersive medium has been computed using the SCN-TLM method [10] by introducing several frequency dependence models (e.g., Drude model, Lorentz model, Debye model, Condon model, Cole-cole model, Davidson-cole model), with different approaches as the Shift-Operator (SO) formulation [11], Piecewise Linear Recursive Convolution (PLRC) approach [12], Runge-Kutta Exponential Time Differencing (RKETD) technique [13], Auxiliary

Received 9 June 2023, Accepted 22 September 2023, Scheduled 4 October 2023
* Corresponding author: Mohamed Moumou (mohamed.moumou@etu.uae.ac.ma).
The authors are with the EMG Group, LaSIT Laboratory, Abdelmalek Essaadi University, Tetouan, Morocco.

Differential Equations (ADE) technique [14, 15], and Piecewise Linear Current Density Recursive Convolution (PLCDRC) formulation [16].

In this article, for the first time, TLM method is used to model and simulate the electromagnetic behaviour of 2D materials generally and graphene sheet specially, and an ADE technique incorporating the intraband conductivity is implemented to numerically model graphene sheet in which voltage sources are added on each TLM node. Our method is validated by numerical simulations for Terahertz applications, and the results are compared with the theoretical ones.

The present article is organized as follows. Section 2 introduces the electronic model of graphene sheet. Formulations and equations are presented in Section 3. Section 4 reports the numerical results and discussions. Finally a conclusion is given in Section 5.

2. ELECTRONIC MODEL OF GRAPHENE SHEET

A single graphene layer is modeled as a thin complex conducting surface. The analytical expression for the surface conductivity of graphene layer can be obtained based on the Kubo formalism in an integral form [17], as follows:

$$\sigma_s(\omega) = \frac{je^2(\omega - j2\Gamma)}{\pi\hbar^2}\left[\frac{1}{(\omega - j2\Gamma)^2}\int_0^\infty \varepsilon\left(\frac{\partial f_d(\varepsilon)}{\partial\varepsilon} - \frac{\partial f_d(-\varepsilon)}{\partial\varepsilon}\right)d\varepsilon - \int_0^\infty \frac{f_d(-\varepsilon) - f_d(\varepsilon)}{(\omega - j2\Gamma)^2 - 4(\varepsilon/\hbar)^2}\,d\varepsilon\right] \quad (1)$$

where $-e$ is the electron charge, ω the angular frequency of the incident wave, Γ the scattering rate, $\hbar = h/2\pi$ the reduced Plank constant, ε the energy of a single-electron state, $f_d(\varepsilon) = 1/[e^{(\varepsilon-\mu_c)/k_BT} + 1]$ the Femi-Dirac distribution function, k_B the Boltzmann constant, T the temperature, and μ_c the chemical potential known also as the Fermi level E_F that can be controlled by chemical doping or electrostatic bias field E_0.

The first term and second term of surface conductivity in Eq. (1) are due to intraband contribution and interband contribution, respectively:

$$\sigma_s(\omega) = \sigma_s^{intra}(\omega) + \sigma_s^{inter}(\omega) \quad (2)$$

when $2|\mu_c| \gg \hbar\omega$, the intraband conductivity dominates; on the other hand, if $2|\mu_c| \leq \hbar\omega$ the interband conductivity becomes dominated [4, 7–9]. In this work, the chemical potential is taken as $|\mu_c| \leq 1\,\text{eV}$, and the terahertz frequency regime is considered. Therefore, the interband term can be neglected, and only the intraband conductivity will be considered and approximated by a Drude model expression, which leads to:

$$\sigma_s(\omega) = \sigma_s^{intra}(\omega) = \frac{\sigma_0}{1 + j\omega\tau} \quad (3)$$

where $\tau = 1/2\Gamma$ is known as the phenomenological electron relaxation time, and σ_0 is the conductivity of frequency independent [Direct current (DC)] and can be defined as:

$$\sigma_0 = \frac{e^2\tau k_BT}{\pi\hbar^2}\left[\frac{\mu_c}{k_BT} + 2Ln\left(e^{-\mu_c/k_BT} + 1\right)\right] \quad (4)$$

Instead of surface conductivity defined in Eq. (3), the volumetric conductivity of a thin graphene layer with thickness h can be evaluated by the following expression as in [18–22]:

$$\sigma_v(\omega) = \frac{\sigma_s^{intra}(\omega)}{h} \quad (5)$$

The volumetric conductivity in Eq. (5) can be implemented in the ADE-TLM formulation and will be used in the next section.

3. FORMULATIONS AND EQUATIONS

Considering an isotropic graphene sheet medium, the Maxwell-Ampere equation in time domain related to the conduction current density can be presented as:

$$\nabla \times \mathbf{H}(t) = \mathbf{J}(t) + \epsilon_0\frac{\partial \mathbf{E}(t)}{\partial t} \quad (6)$$

where ϵ_0 is the dielectric constant of free space, $\mathbf{E}$ the electric field vector, $\mathbf{H}$ the magnetic field vector, and $\mathbf{J}$ the conduction current density vector.

The constitutive relation in frequency domain related $\mathbf{J}$ and $\mathbf{E}$ in the graphene sheet medium is defined as:

$$\mathbf{J}(\omega) = \sigma_v(\omega)\mathbf{E}(\omega) \tag{7}$$

Suppose that graphene layer is located in the xy plane, excited by a normally incident plane wave, polarized along u-direction, Eq. (6) and Eq. (7) can be rewritten as:

$$\frac{\partial E_u(t)}{\partial t} = \frac{1}{\epsilon_0}\left[-J_u(t) + (\nabla \times H(t))_u\right] \tag{8}$$

and

$$J_u(\omega) = \sigma_v(\omega)E_u(\omega) \tag{9}$$

where $u \in \{x, y\}$.

By substituting Eq. (5) into Eq. (9), we arrive at:

$$J_u(\omega) = \frac{\sigma_0/h}{1 + j\omega\tau}\, E_u(\omega) \tag{10}$$

where $\sigma_{0_h} = \frac{\sigma_0}{h}$.

Then

$$(1 + j\omega\tau)J_u(\omega) = \sigma_{0_h}E_u(\omega) \tag{11}$$

Converting Eq. (11) from frequency domain to time domain, and for the case of harmonic fields ($j\omega \equiv \frac{\partial}{\partial t}$), we have:

$$J_u(t) + \tau\frac{\partial J_u(t)}{\partial t} = \sigma_{0_h}E_u(t) \tag{12}$$

By applying the time domain central difference approximation scheme at step n, we can obtain:

$$\frac{J_u^{n+\frac{1}{2}} + J_u^{n-\frac{1}{2}}}{2} + \tau\frac{J_u^{n+\frac{1}{2}} - J_u^{n-\frac{1}{2}}}{\Delta t} = \sigma_{0_h}E_u^n \tag{13}$$

$$\left[\frac{1}{2} + \frac{\tau}{\Delta t}\right]J_u^{n+\frac{1}{2}} + \left[\frac{1}{2} - \frac{\tau}{\Delta t}\right]J_u^{n-\frac{1}{2}} = \sigma_{0_h}E_u^n \tag{14}$$

$$(\Delta t + 2\tau)\left(J_u^{n+1} + J_u^n\right) + (\Delta t - 2\tau)\left(J_u^n + J_u^{n-1}\right) = 4\sigma_{0_h}\Delta t E_u^n \tag{15}$$

After some operations, the expression of J_u^{n+1}:

$$J_u^{n+1} = \left[\frac{2\tau - \Delta t}{2\tau + \Delta t} - 1\right]J_u^n + \left[\frac{2\tau - \Delta t}{2\tau + \Delta t}\right]J_u^{n-1} + \left[\frac{4\sigma_{0_h}\Delta t}{2\tau + \Delta t}\right]E_u^n \tag{16}$$

where $\alpha = \frac{2\tau - \Delta t}{2\tau + \Delta t}$, and $\beta = \frac{4\sigma_{0_h}\Delta t}{2\tau + \Delta t}$.

Finally, the update equation for conduction current density J_u component is derived:

$$J_u^{n+1} = (\alpha - 1)J_u^n + \alpha J_u^{n-1} + \beta E_u^n \tag{17}$$

For the electric field component E_u update equation, the central difference approximation of Maxwell Ampere Eq. (8) centered at step $n + \frac{1}{2}$ can be written as:

$$\left[\frac{E_u^{n+1} - E_u^n}{\Delta t}\right] = \frac{1}{\epsilon_0}\left[-J_u^{n+\frac{1}{2}} + [\nabla \times H]_u^{n+\frac{1}{2}}\right] \tag{18}$$

$$E_u^{n+1} = E_u^n - \frac{\Delta t}{\epsilon_0}J_u^{n+\frac{1}{2}} + \frac{\Delta t}{\epsilon_0}[\nabla \times H]_u^{n+\frac{1}{2}} \tag{19}$$

The conduction current density component J_u at step $n + \frac{1}{2}$ can be approximated by:

$$J_u^{n+\frac{1}{2}} = \frac{J_u^{n+1} + J_u^n}{2} \tag{20}$$

By substituting Eq. (17) in Eq. (20) we get:

$$J_x^{n+\frac{1}{2}} = \frac{\alpha(J_u^n + J_u^{n-1}) + \beta E_u^n}{2} \tag{21}$$

And we substitute Eq. (21) into Eq. (19) to obtain:

$$E_u^{n+1} = E_x^n - \frac{\Delta t}{2\epsilon_0}\left[\alpha(J_u^n + J_u^{n-1}) + \beta E_u^n\right] + \frac{\Delta t}{\epsilon_0}\left[\nabla \times H\right]_u^{n+\frac{1}{2}} \tag{22}$$

Then the updated equation for the electric field component E_u can be obtained as follows:

$$E_u^{n+1} = E_u^n - \frac{\alpha\Delta t}{2\epsilon_0}\left(J_u^n + J_u^{n-1}\right) - \frac{\beta\Delta t}{2\epsilon_0} E_u^n + \frac{\Delta t}{\epsilon_0}\left[\nabla \times H\right]_u^{n+\frac{1}{2}} \tag{23}$$

In order to get the set of specific equation to the TLM formalism, the analogy between total electric voltage V_u on transmission line and electric field component of EM wave has been established at the center of the node for a uniform (SCN)TLM mesh as follows [23]:

$$E_u = \frac{V_u}{\Delta l} \tag{24}$$

where Δl is the TLM mesh width.

The update equation of J_u component from Eq. (17) can be write as:

$$J_u^{n+1} = (\alpha - 1)J_u^n + \alpha J_u^{n-1} + \frac{\beta}{\Delta l} V_u^n \tag{25}$$

And the update equation of total electric voltage V_u from Eq. (23) becomes:

$$V_u^{n+1} = V_u^n - \frac{\alpha\Delta t\Delta l}{2\epsilon_0}\left(J_u^n + J_u^{n-1}\right) - \frac{\beta\Delta t}{2\epsilon_0} V_u^n + \frac{\Delta t\Delta l}{\epsilon_0}\left[\nabla \times H\right]_u^{n+\frac{1}{2}} \tag{26}$$

According to the same methodology as in the ADE-(SCN)TLM approach [14, 15], we get the normalized admittance of the open circuit capacitive stub added to the standard SCN-TLM node and the update equation for voltage source which model electrical dispersive behavior of graphene sheet.

We can define the normalized admittance in u direction for the node, and it can be expressed as:

$$Y_{oc,u} = 0 \quad \text{with} \quad u \in \{x, y\} \tag{27}$$

The voltage source update equation in u direction at the center of the node is found to be:

$$V_{s,u}^{n+1} = -V_{s,u}^n - \frac{2\alpha\Delta t\Delta l}{\epsilon_0}\left(J_u^n + J_u^{n-1}\right) - \frac{2\beta\Delta t}{\epsilon_0} V_u^n \tag{28}$$

which can be written in the form:

$$V_{s,u}^{n+1} = -V_{s,u}^n + Q\left[J_u^n + J_u^{n-1}\right] + RV_u^n \tag{29}$$

where $Q = -\frac{2\alpha\Delta t\Delta l}{\epsilon_0}$ and $R = -\frac{2\beta\Delta t}{\epsilon_0}$.

By the application of electric field continuity and electric charge conservation laws [23] to the standard SCN-TLM characterized by 12 ports, with additional ports of voltage source injected in port 13 or 14, the expression of the final total voltages V_u update equation in the center of the node becomes:

$$V_u^{n+1} = V_{x,y}^{n+1} = \frac{1}{2}\left[V_{1,3}^i + V_{2,4}^i + V_{9,8}^i + V_{12,11}^i\right]^{n+1} + \frac{1}{4}\left[V_{13,14}\right]^{n+1} \tag{30}$$

where

$$\begin{pmatrix} V_{13}^i \\ V_{14}^i \end{pmatrix}^{n+1} = \begin{pmatrix} V_{s,x} \\ V_{s,y} \end{pmatrix}^{n+1}$$

From the above, the implementation process of the ADE-(SCN)TLM is given as:

1) J_u^{n+1} component is obtained from Eq. (25);

2) $V_{s,u}^{n+1}$ component is calculated from Eq. (29);

3) E_u^{n+1} component is computed from Eq. (24) and Eq. (30);

4) Finally, scattering process and connecting process are determined by employing the scattering matrix, and the connexion matrix, respectively, as in [13].

4. NUMERICAL RESULTS AND DISCUSSIONS

To investigate the effectiveness and validity of the ADE-TLM method proposed above for an isotropic graphene sheet medium with the external electrostatic E_0 biasing field in the direction of propagation along z-axis, the interaction of an electromagnetic wave in normal incidence with a graphene slab is simulated. The network is subdivided into $(1 \times 1 \times 300)\Delta t$, with the mesh width $\Delta l = h = \Delta x = \Delta y = \Delta z = \lambda_{\min}/20$ as in [24, 25], $\Delta l = 1.5\,\mu\text{m}$, where $\lambda_{\min}$ is the minimum wavelength corresponding to the highest frequency of interest $f_{\max} = 10\,\text{THz}$. The graphene slab occupies the cell number 150, while the rest of computational domain is vacuum. Two observation points are located from one cell on each side of the graphene sheet to calculate the electric fields. Absorbant Boundary Condition (ABC) of 1 cell at both ends of the z-direction is used to truncate the domain. A periodic boundary condition (PBC) is used along the x and y directions to simulate an infinite graphene sheet. The physical parameters of

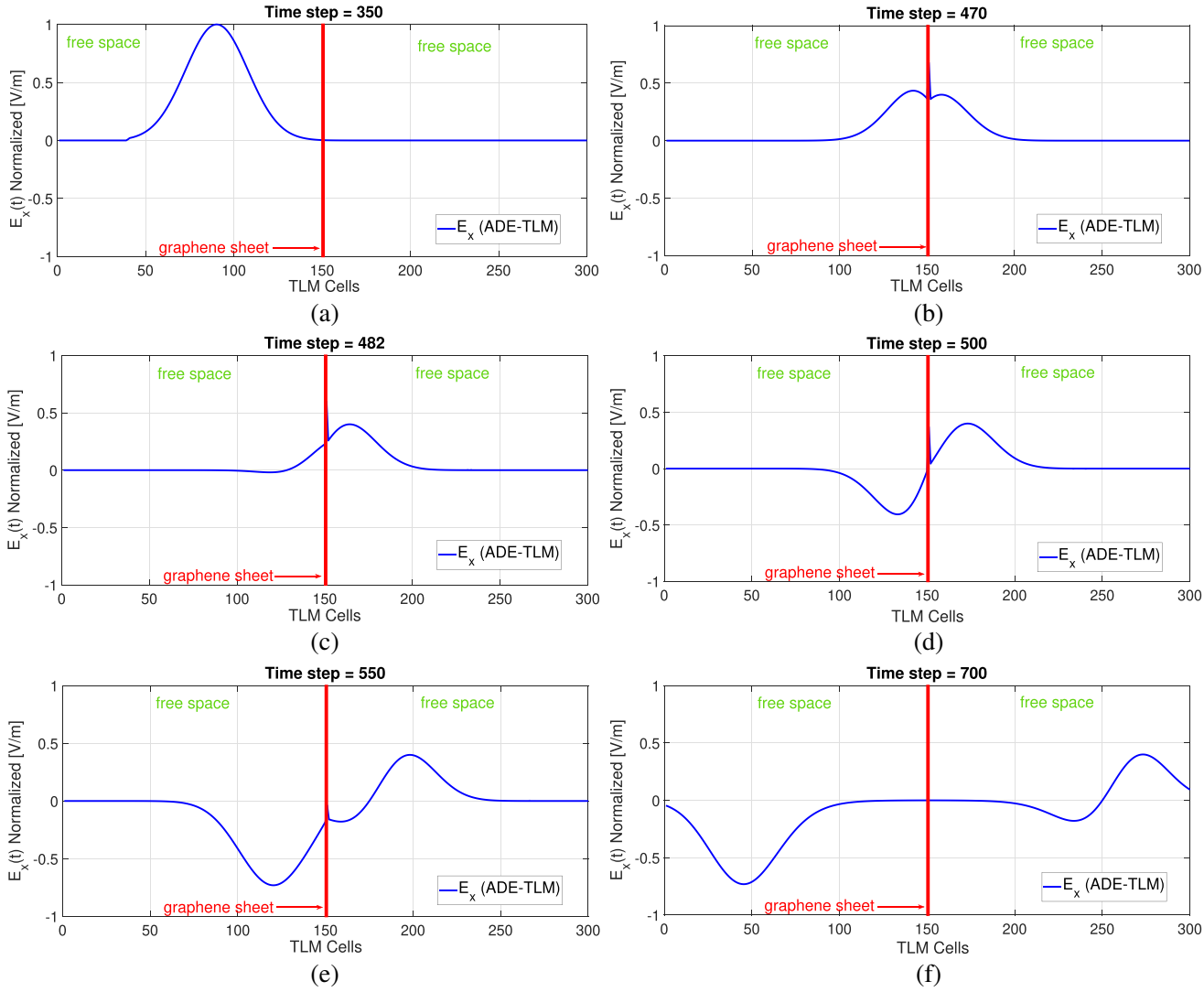

Figure 1. Snapshot of the total normalized electric field obtained by the proposed method, propagates in vacuum and strikes graphene slab in different time steps, (a) propagation of incident E_x at time step 350, (b) propagation of transmitted and reflected E_x at time step 470, (c) propagation of transmitted and reflected E_x at time step 482, (d) propagation of transmitted and reflected E_x at time step 500, (e) propagation of transmitted and reflected E_x at time step 550, (f) propagation of transmitted and reflected E_x at time step 700.

graphene in the structure are as follows: $\tau = 0.3\,\text{ps}$, $T = 300\,\text{K}$, and $\mu_c = 0.7\,\text{eV}$. The structure is excited by normally incident Gaussian pulse plane wave: $E_x^{inc}(t) = e^{-[t-t_0]^2/\tau^2}$, with duration $\tau = 50\Delta t$, and delay $t_0 = 5\tau$, polarized along x-direction generated in the cell number 40. The simulation is performed for 2000 iterations corresponding to a total time of 5 ps.

The evolution of the Gaussian pulse using the ADE-TLM approche is depicted in Fig. 1(a) which illustrates the propagation of incident electric pulse after 350 iterations in the vacuum with only E_x component. After penetration in the graphene slab, both E_x components reflected and transmitted appear as shown in (b) 470^{th} snapshot, (c) 482^{th} snapshot, (d) 500^{th} snapshot, (e) 550^{th} snapshot, and (f) 700^{th} snapshot. Since the incident Gaussian wave is polarized in the x direction, the transmitted and reflected waves are also polarized in the same direction. It can be seen that there is no instability observed during the whole time period.

The transmission (T) and reflection (Γ) coefficients are significant parameters in the propagation characteristics of EM fields. By applying the Fast Fourier Transform (FFT) to calculate the electric fields on both observation points, the magnitudes and phases of T and Γ are derived numerically as illustrated in Fig. 2 and compared to the exact solution calculated by $T = 2/(2 + \eta_0\sigma_s^{intra})$ and $\Gamma = T - 1$ [17, 26], where $\eta_0 = 120\pi\Omega$ is the intrinsic impedance of free space. It is found that the computed results and the analytic solutions are in good agreement.

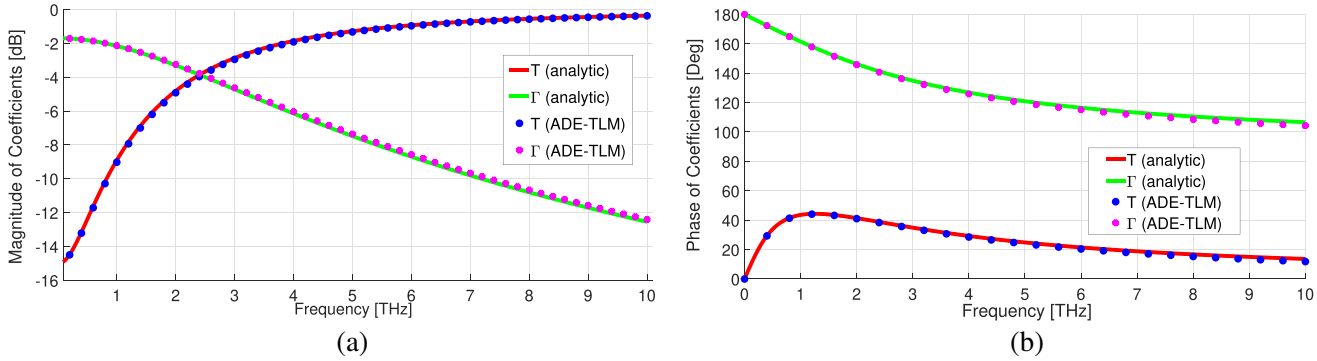

Figure 2. Transmission and reflection coefficients (a) magnitude, (b) phase.

To study the effect of chemical potential on the behavior wave propagation through graphene sheet, the parameters of graphene sheet remain unchanged as in the previous simulation while varying the chemical potential $\mu_c(E_0)$ in the direction of propagation from 0.1 eV to 0.9 eV. Fig. 3 demonstrates the transmission coefficients versus frequency for different electrostatic fields. The transmission coefficients start from different minimum values at the same frequency, and the bandwidth increases with the increase of the biased electrostatic field. This tunable parameter can be used to control the bandwidth precisely. It can also be seen that all the calculated lines and analytical ones match well.

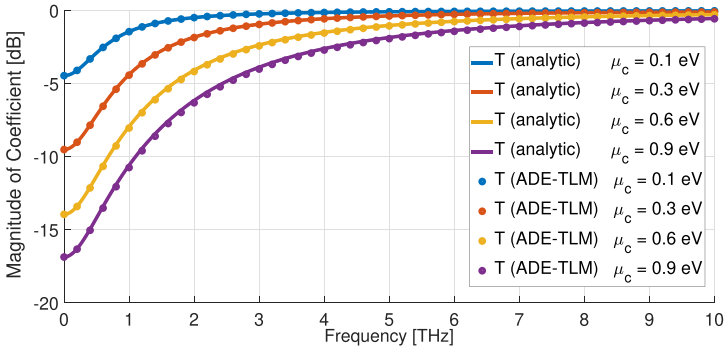

Figure 3. Transmission coefficient versus frequency for different biased electrostatic fields.

5. CONCLUSION

In this article, we propose a new TLM algorithm to model and simulate EM wave propagation in a graphene sheet, which is based on Symmetrical Condensed Node (SCN), Auxiliary Differential Equation (ADE) technique, and the introduction of voltage source which model electrical dispersive properties of the medium. Validation of the method is achieved through numerical examples. The obtained results have been compared with the analytical solutions and prove that the proposed method is stable and has an excellent accuracy. The transmission coefficients can be controlled by changing the biased electrostatic field and can be used to model and simulate graphene-based complex devices such as filter, reflector, antenna, and sensor, for frequencies below the THz frequency regime [27].

REFERENCES

1. Mbayachi, V. B., E. Ndayiragije, T. Sammani, S. Taj, and E. R. Mbuta, "Graphene synthesis, characterization and its applications: A review," *Results in Chemistry*, Vol. 3, 100163, 2021.
2. Yang, G., L. Li, W. B. Lee, and M. C. Ng, "Structure of graphene and its disorders: A review," *Science and Technology of Advanced Materials*, Vol. 19, No. 1, 613–648, 2018.
3. Kumar, V., "Linear and nonlinear optical properties of graphene: A review," *Journal of Electronic Materials*, Vol. 50, No. 7, 3773–3799, 2021.
4. Ramadan, O., "Improved direct integration auxiliary differential equation FDTD scheme for modeling graphene drude dispersion," *Optik*, Vol. 219, 165173, 2020.
5. Wang, D. W., W. S. Zhao, X. Q. Gu, W. Chen, and W. Y. Yin, "Wideband modeling of graphene-based structures at different temperatures using hybrid FDTD method," *IEEE Transactions on Nanotechnology*, Vol. 14, No. 2, 250–258, 2015.
6. Moharrami, F. and Z. Atlasbaf, "Simulation of multilayer graphene-dielectric metamaterial by implementing SBC model of graphene in the HIE-FDTD method," *IEEE Transactions on Antennas and Propagation*, Vol. 68, No. 3, 2238–2245, 2019.
7. Chen, W.-J., Q.-W. Liang, S.-Y. Long, and M. Zhao, "Modeling thin graphene sheets in the WLP-FDTD algorithm with surface boundary condition," *Progress In Electromagnetics Research Letters*, Vol. 91, 93–98, 2020.
8. Sarker, P. C., M. M. Rana, and A. K. Sarkar, "Modeling of graphene conductivity using FDTD in the near infrared frequency," *2nd International Conference on Electrical, Computer & Telecommunication Engineering (ICECTE)*, 2016.
9. Hossain, M. B., S. Muktadhir, and M. M. Rana, "Multi-structural optical devices modeling using graphene tri-layer sheets," *Optik*, Vol. 127, No. 15, 5841–5851, 2016.
10. Johns, P. B., "A symmetrical condensed node for the TLM method," *IEEE Transactions on Microwave Theory and Techniques*, Vol. 35, No. 4, 370–377, 1987.
11. El Adraoui, S., K. Mounirh, M. I. Yaich, and M. Khalladi, "Shift operator-TLM method for modeling gyroelectric media," *Progress In Electromagnetics Research M*, Vol. 87, 189–197, 2019.
12. El Adraoui, S., A. Zugari, M. Bassouh, M. I. Yaich, and M. Khalladi, "Novel PLRC-TLM algorithm implementation for modeling electromagnetic wave propagation in gyromagnetic media," *Methodology*, Vol. 6, No. 1, 2013.
13. El Adraoui, S., M. Bassoh, M. Khalladi, M. I. Yaich, and A. Zugari, "RKETD-TLM modeling of anisotropic magnetized plasma," *International Journal of Science and Advanced Technology*, Vol. 2, No. 8, 81–84, 2012.
14. Mounirh, K., S. El Adraoui, Y. Ekdiha, M. I. Yaich, and M. Khalladi, "Modeling of dispersive chiral media using the ADE-TLM method," *Progress In Electromagnetics Research M*, Vol. 64, 157–166, 2018.
15. Kanjaa, M., K. Mounirh, S. El Adraoui, O. El Mrabet, and M. Khalladi, "An ADE-TLM modeling of biological tissues with cole-cole dispersion model," *Progress In Electromagnetics Research M*, Vol. 89, 161–169, 2020.

16. Mounirh, K., S. El Adraoui, M. Charif, M. I. Yaich, and M. Khalladi, "Modeling of anisotropic magnetized plasma media using PLCDRC-TLM method," *Optik*, Vol. 126, Nos. 15–16, 1479–1482, 2015.
17. Hanson, G. W., "Dyadic Green's functions and guided surface waves for a surface conductivity model of graphene," *Journal of Applied Physics*, Vol. 103, No. 6, 064302, 2008.
18. Wang, X. H., J. Y. Gao, and F. L. Teixeira, "Stability-improved ADE-FDTD method for wideband modeling of graphene structures," *IEEE Antennas and Wireless Propagation Letters*, Vol. 18, No. 1, 212–216, 2018.
19. Niu, K., P. Li, Z. Huang, L. J. Jiang, and H. Bagci, "Numerical methods for electromagnetic modeling of graphene: A review," *IEEE Journal on Multiscale and Multiphysics Computational Techniques*, Vol. 5, 44–58, 2020.
20. Kim, Y. H., H. Choi, J. Cho, and K. Y. Jung, "FDTD modeling for the accurate electromagnetic wave analysis of graphene," *Journal of Electrical Engineering and Technology*, Vol. 15, 1281–1286, 2020.
21. Sarker, P. C., M. M. Rana, and A. K. Sarkar, "A simple FDTD approach for the analysis and design of graphene based optical devices," *Optik*, Vol. 144, 1–8, 2017.
22. Shao, Y., J. J. Yang, and M. Huang, "A review of computational electromagnetic methods for graphene modeling," *International Journal of Antennas and Propagation*, Vol. 2016, 2016.
23. Christopoulos, C., "The transmission-line modeling (TLM) method in electromagnetics," *Synthesis Lectures on Computational Electromagnetics*, Vol. 1, No. 1, 1–132, 2005.
24. Bouzianas, G. D., N. V. Kantartzis, C. S. Antonopoulos, and T. D. Tsiboukis, "Optimal modeling of infinite graphene sheets via a class of generalized FDTD schemes," *IEEE Transactions on Magnetics*, Vol. 48, No. 2, 379–382, 2012.
25. Wang, X. H., W. Y. Yin, and Z. Chen, "Matrix exponential FDTD modeling of magnetized graphene sheet," *IEEE Antennas and Wireless Propagation Letters*, Vol. 12, 1129–1132, 2013.
26. Afshar, F., A. Akbarzadeh-Sharbaf, and D. D. Giannacopoulos, "A provably stable and simple FDTD formulation for electromagnetic modeling of graphene sheets," *IEEE Transactions on Magnetics*, Vol. 52, No. 3, 1–4, 2015.
27. El Jbari, M. and M. Moussaoui, *High-performance Metric of Graphene-based Heterojunction LEDs and PDs in Visible Light Communication Systems, Recent Advances in Graphene Nanophotonics*, Springer Nature, Cham, Switzerland, 2023.